EJGE

Comparison of Different Probabilistic Methods for Analyzing Stability of Underground Rock Excavations

Musa Adebayo Idris

Lecturer
Department of Mining Engineering,
School of Engineering and Engineering Technology,
Federal University of Technology, Akure, Nigeria
e-mail: maidris@futa.edu.ng

Researcher
Division of Mining and Geotechnical Engineering,
Luleå University of Technology ,SE-971 87 Luleå, Sweden
e-mail: idris.musa@ltu.se

Erling Nordlund

Professor
Division of Mining and Geotechnical Engineering,
Luleå University of Technology ,SE-971 87 Luleå, Sweden
e-mail: erling.nordlund@ltu.se

David Saiang

Associate Professor
Division of Mining and Geotechnical Engineering,
Luleå University of Technology ,SE-971 87 Luleå, Sweden
e-mail: david.saiang@ltu.se

ABSTRACT

Stability analyses of underground rock excavations are often performed using traditional deterministic methods. In deterministic methods the mean or characteristics values of the input parameters are used for the analyses. These method neglect the inherent variability of the rock mass properties in the analyses and the results could be misleading. Therefore, for a realistic stability analyses probabilistic methods, which consider the inherent variability of the rock mass properties, are considered appropriate. A number of probabilistic methods, each based on different theories and assumptions have been developed for the analysis of geotechnical problems. Geotechnical engineers must therefore choose appropriate probabilistic method to achieve a specific objective while taking into account simplicity, accuracy and time efficiency. In this study finite difference method was combined with five different probabilistic methods to analyze the stability of an underground rock excavation. The probabilistic methods considered were the Point Estimate Method (PEM), the Response Surface Method (RSM), the Artificial Neural Network (ANN), the Monte Carlos Simulation (MCS), and the Strength Classification Method (SCM). The results and the relative merits of the methods were compared. Also the general advantages of the probabilistic method over the deterministic method were discussed. Though the methods presented in this study are not exhaustive, the results of this study will assist in the choice of appropriate probabilistic methods for the analysis of underground rock excavations.

KEYWORDS: Probabilistic methods, rock mass property variability, underground rock excavation stability.

INTRODUCTION

As a result of underground construction in rock, the original state of the hosting rock mass is disturbed. This disturbance may lead to instability of the excavation which would pose a threat to the safety of personnel and equipment in and around such an excavation. The stability of underground excavations has, therefore, always been of major concern to geotechnical engineers.

The stability of underground excavations depends on such factors as: the mechanical properties of the rock mass, the orientation and properties of the rock discontinuities, the hydrological conditions and the induced stresses [1]. In the stability analysis these parameters are determined either by in situ investigations or laboratory tests. Because of the inherent uncertainties associated with natural materials such as rock masses, the exact values for these parameters cannot be determined as the values vary within a certain range [2].

The main sources of uncertainties are inherent random heterogeneity (spatial variability or aleatory uncertainty) and knowledge-based or epistemic uncertainties, that is to say measurement error and transformation uncertainties [3]. The in situ variability or aleatory uncertainty stems from natural transformation processes such as diagenesis, fractional crystallization and metamorphism that affect the physical and mechanical properties of the geotechnical materials [4]. Measurement error arises from human error and equipment errors during data collection and measurement while the transformation uncertainty or model uncertainty may be attributed to the transformation of field or laboratory data into geotechnical design parameters using empirical equations.

If uncertainty in the geotechnical parameters is not properly considered, it can significantly affect the results from analysis of underground excavations. With regard to geotechnical engineering problems these uncertainties are sometimes accounted for by considering the best, mean and worst cases of the material inputs for the analysis. This approach, however, does not give a clear understanding of the compound effects of the input uncertainties. Therefore, for a realistic analysis of underground excavations the compound effects of the uncertainties in the input parameters must be adequately considered using probabilistic methods. Probabilistic methods provide a rational basis for considering the uncertainties in the geotechnical analysis. Several probabilistic methods have been used for geotechnical analysis, though majorly of surface geotechnical structures such as slopes and embankments. Probabilistic methods have also been used to analyze underground rock excavations [4 – 13].

The probabilistic methods used in the geotechnical analyses employ different statistical tools and assumptions. According [14] the probabilistic methods can be divided into two categories: analytical approximation methods (e.g., the first-order second moment method) and sampling based methods. Analytical approximation methods may not be suitable for the assessment of geotechnical problems that involve numerical modeling since they require explicit functions which are not readily available or which are difficult to apply to complex geotechnical problems. Sampling based methods could use discrete or random sampling (simulation based). The discrete sampling methods such as the Point Estimate Methods (PEM), the Response Surface Method (RSM) and the Artificial Neural Network (ANN) assume that the scale of the variability is large compared to the domain of the problem being considered such that the domain (i.e. the rock mass) can be treated as homogenous. When the scale of the variability is small then the variability has to be treated as heterogeneous. In that case simulation based methods such as the Monte Carlo Simulation (MCS) would be most appropriate to use. With the simulation based sampling methods the heterogeneity of the rock mass can be explicitly considered in the numerical modeling.

Since different probabilistic methods utilize different theories and assumptions, one of the problems that could hamper the application is the choice of probabilistic method to achieve a specific objective while considering simplicity, accuracy and minimum computational time. Therefore in this paper, the finite difference method (FDM) is combined with different probabilistic methods to analyze the stability of a drift in a good quality rock mass conditions. The probabilistic methods considered are the PEM, the RSM, the ANN, the MCS and the Strength Classification Method (SCM). The PEM, the RSM and the ANN assume a homogenous rock mass while the MCS and the SCM incorporate both variability and heterogeneity of the rock mass properties into the numerical stability analysis of an underground excavation. The results from the methods were compared and the relative merits and shortcomings of each method discussed.

PROBABILISTIC METHODS

In most rock masses the uncertainty in their properties is so great that cannot be ignored. Probabilistic methods need therefore to be applied. In this section, the different probabilistic methods used in this paper are briefly explained. These probabilistic methods were divided into two categories based on their sampling methods and assumptions – those methods that consider the heterogeneity of the rock mass and those which do not consider the heterogeneity.

Methods neglecting rock mass heterogeneity

For the purpose of this study, the Point Estimate Method (PEM), the Response Surface Method (RSM) and the Artificial Neural Network (ANN) were considered.

Point Estimate method (PEM)

The PEM was originally proposed by [15] for symmetric variables and revised in 1981 [16] to also include asymmetric variables. According to [17] the PEM is a special case of the Gaussian quadrature. In the PEM, the statistical moments of a function are approximated from the random variables by replacing the probability density functions (PDFs) of each of the random variables with probability mass functions (PMFs) consisting of a few discrete points, typically two points. In the two point estimate method, 2^n estimations are needed when there are n correlated or uncorrelated random variables with symmetric distribution. The two points of estimation are chosen at ± one standard deviation from the mean value for each distribution. Furthermore, each point of estimation has a weighting value which depends on the correlation between the variables. For uncorrelated variables, each point of estimation will be weighted equally with the value 2^{-n}.

A great limitation of the original PEM is that when large numbers of random variables are involved in the analysis the number of estimations becomes too large for practical application. For this reason, modifications of the PEM to reduce the number of the sampling points have been proposed by e.g. [18 – 21]. However, according to [22] these modifications move the weighting points further away from the mean values as the number of variables increases. This can lead to input values that extend beyond the valid domain. Due to this problem, the original Rosenblueth PEM is often used with fewer random variables. The PEM is widely used together with numerical methods in geotechnical engineering because of its simplicity [6, 9, 13, 23].

Response surface method (RSM)

The RSM is a collection of mathematical and statistical techniques used to develop a functional relationship between a dependent output y and a number of associated input variables (x_1, x_2,..x_n). This relationship is implicit in most geotechnical engineering problems and is generally an unknown. However, it can be approximated by a low-degree polynomial model of the form:

$$y = f(x_1, x_2, ...x_n) + \varepsilon \quad (1)$$

where ε is the error observed in the output y and $f(x_1, x_2, ...x_n)$ is called the response surface. The most common response surfaces used in geotechnical engineering problems are low-order polynomials (first-order and second-order models). If the output can be well modeled by a linear function then the first-order model is used: otherwise the second-order model is used. A general first-order model is defined as:

$$y = a_0 + a_1 x_1 + a_2 x_2 + ... + a_n x_n + \varepsilon \quad (2)$$

and the general second-order model with interacting terms is defined as:

$$y = a_0 + \sum_{i=1}^{n} a_i x_i + \sum_{i=1}^{n} a_{ii} x_i^2 + \sum_{i=1}^{n} \sum_{j=1, i<j}^{n} a_{ij} x_i x_j + \varepsilon \quad (3)$$

where a_i are the regression coefficients and n is the number of basic input variables.

In the RSM analysis 2^n full factorial design is used to fit the first order linear regression. For the second order quadratic regression, at least $\frac{(n+1)(n+2)}{2}$ evaluation points are needed to fit the polynomial. RSM has been used in combination with numerical analysis to assess the stability of underground rock excavations [8, 12].

Artificial Neural Network (ANN)

The ANN is a form of artificial intelligence that attempts to imitate the behavior of the human brain and nervous system. The ANN can be used to capture the relationship between a set of inputs and outputs, which are not sufficiently known, by means of training the data obtained from either real experiments or numerical simulations [24]. The ANN has been applied in the stability analysis of tunnels and underground excavations by, for example, [25 – 29]. In principle, the ANN consists of simple interconnected nodes or neurons where p is the input, *w* is the weight, *b* is the bias, *f* is the transfer function and a is the output.

If the neuron has *N* number of inputs then the output a can be calculated as:

$$a = f\left(\sum_{i=1}^{N} w_i p_i + b\right). \quad (4)$$

Different types of transfer functions can be used in the ANN such as hard limit, linear and log-sigmoid transfer functions [30]. The choice of transfer function depends on the specification of the problem that the neuron is attempting to solve [30].

The architecture of the ANN consists of the number of layers, the number of neurons in each layer and the neuron transfer functions. Two or more neurons can be combined in a layer and a network could contain one or two layers whereby each layer has different roles. There is always one output layer and one input layer while there can be many hidden layers for an ANN. However, it is known that a network with one hidden layer can approximate any continuous function provided with sufficient connection weights [31]. The number of neurons in the input and output layers are determined by the number of the model input and output variables. There is no any exact guide for determining the number of neurons in the hidden layer [32]. However some researchers e.g. [33 - 35] have proposed heuristic relations for determining the neuron size.

Before an ANN can be used to make projections or predictions it has to be trained. In the training or learning process, the network is presented with a pair of training datasets including input and the corresponding target values. The network computes its own output using its initial weights and biases. Then, the weights and biases are adjusted iteratively to reduce the errors between the network output and the target output. Mean square error is used as error index during the training phase to improve the network performance [36]. One of the most commonly used learning algorithms in geotechnical engineering is the back-propagation algorithm (BPA) proposed by [37]. In the BPA there are two phases: forward prediction which calculates the output values of the ANN from training data and error back-propagation which adjusts the weight. There are many techniques to adjust the error but the steepest descent method is often used [36]. Once the training process of the ANN is completed predictions can be made for a new input dataset.

Methods considering rock mass heterogeneity

As mentioned previously the basic assumption of the methods in Section 2.1 is that the properties of the geotechnical domain being analyzed can be treated as homogeneous. However, this assumption may affect the results of the analysis especially when the natural variability (i.e. heterogeneity) of the geotechnical parameters is more profound. Hence, the Monte Carlo Simulation (MCS) technique is often employed to model the natural randomness or heterogeneity. The MCS requires a large number of simulations to achieve the required level of accuracy and because of this there have been some modifications to the sampling techniques of the MCS in order to reduce the number of the simulations or the computational time. Two examples of alternatives to the MCS are the Latin Hyper Cube (LHC) techniques and the Strength Classification Method (SCM) [38]. For this study the MCS and the SCM are considered as the methods which consider the heterogeneity.

Monte Carlo simulation (MCS)

In geotechnical analysis the MCS can be used to obtain the probability distribution of dependent random variables given the probabilistic distribution of the independent random variables. The MCS is considered a powerful tool as it can accurately cover the entire distribution of all uncertain parameters. In another application, the MCS can be utilized to explicitly introduce the rock mass heterogeneity into numerical models by randomly assigning different material properties to each zone of the model based on their probability distribution. In this case, each zone of the model is considered as a “grain” of the rock mass fabric. The locations and combinations of the input variables randomly assigned in the model are different for each simulation. The main disadvantage of the MCS is that it requires many simulations in order to achieve desired accuracy. However, few Monte Carlo simulations can be used to approximate the statistical moments of the output variables [39].

Strength Classification method (SCM)

The strength classification method is a modified form of the MCS with the aim of reducing the computation time. For the SCM the probability density function (e.g. normal distribution) for each random input parameter can be divided or partitioned into a number of classes or groups of different intervals. The PDF can be approximated with histogram as shown in Figure 1 where the width of the rectangle of the histogram represents each of the interval or group. The probability of a random value X of the input parameter within the interval (a, b) can be calculated as

$$P(a < X \leq b) = \int_a^b f_X(x)dx \tag{5}$$

where $f_X(x)$ is the probability distribution function (PDF). For a normally distributed input the probability that a random value of the input parameter is within the interval ($\mu - \sigma$ and $\mu + \sigma$), ($\mu - 2\sigma$ and $\mu + 2\sigma$) and ($\mu - 3\sigma$ and $\mu + 3\sigma$) is 68.3%, 95.4% and 99.7%, respectively. The mean and the standard deviation of the random value are μ and σ, respectively.

The SCM can also be used to introduce heterogeneity of the material properties into a numerical model. The zones in the model will randomly be assigned properties from the classes according to their probabilities, for instance *N* % of the zones will get properties corresponding to the class or group of the input parameter with *N* % probability. The middle value of the interval can be used to represent the random input variables for each class or group. Similar to the MCS, the location of each input variable is randomly varied at each realization of the numerical simulation. Similar to MCS the SCM requires many simulations to achieve the required accuracy.

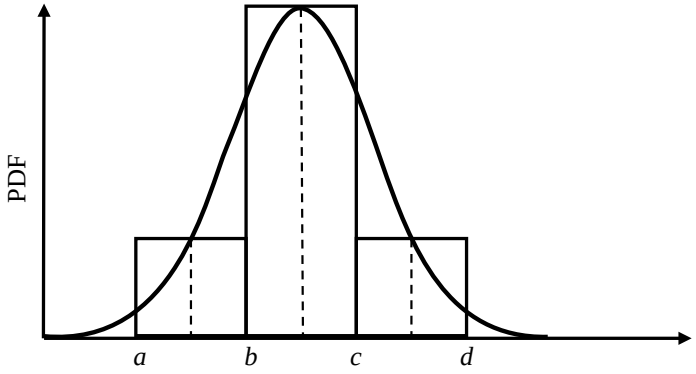

Figure 1: Probability density function partitioned into different intervals

PROBABILISTIC ANALYSIS OF DRIFT STABILITY IN GOOD QUALITY HARD ROCK MASS

To implement and compare the aforementioned probability methods, the stability of a drift in a good quality rock mass, but with varying properties, was investigated.

Problem description and model parameters

An underground mine drift (Figure 2) which has an arched roof and a width and height of 7 m is excavated in a rock mass at a depth of 1000 m. The basic statistical parameters for the rock mass properties are listed in Table 1. The statistical parameters and the distributions of the rock mass parameters are based on the published data in [6, 9, 40, 41]. The minimum and maximum values for the parameters were taken at 95% confidence interval (*CI*). The rock mass behavior is described by an elastic-perfectly plastic model.

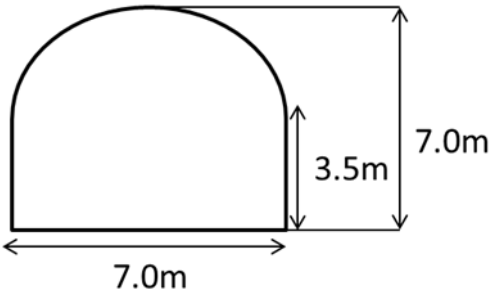

Figure 2: Geometry of the drift

Table 1: Statistical parameters for the rock mass

Parameters	Mean	COV (%)	Max.	Min.
UCS (MPa)	150	15	195	106
GSI	75	10	90	60
m_i	25	10	30	20
Poisson's ratio (v)	0.2	-	-	-
Density (ρ)	2700	-	-	-

The mean values and the coefficient of variation (COV) for the UCS, GSI and m_i together with their respective truncated distributions were used as inputs in the empirical equations proposed by [42, 43] to generate the distribution and statistical parameters of the deformation modulus (E_m), the tensile strength and the equivalent shear strength parameters (i.e. cohesion and internal friction angle). The Monte Carlo technique available in the Excel add-in program @RISK [44] was used for this purpose. Table 2 shows the statistical parameters; mean (μ) and standard deviation (σ), for the deformation modulus (E_m), the tensile strength (σ_t), the cohesion (c) and the internal friction angle (ϕ).

Table 2: Statistical parameters for the deformation modulus (E_m), tensile strength and the equivalent shear strength parameters for the rock mass

Parameters	Mean	σ	Distribution
E_m (GPa)	50.00	14.05	Normal
c (MPa)	4.10	1.64	Normal
σ_t (MPa)	1.03	0.51	Normal
Φ(°)	65.13	0.90	Normal

As the drift will be excavated at a depth of 1000 m the in-situ stresses can be determined from the equations proposed by [45] which are based on over-coring measurements. These are:

$$\sigma_v = \gamma z \tag{5}$$

$$\sigma_H = 6.7 + 0.044z \tag{6}$$

$$\sigma_h = 0.8 + 0.034z \tag{7}$$

where σ_v is the vertical stress, σ_H is the maximum horizontal stress, and σ_h is the minimum horizontal stress. γ, z are the unit weight and depth, respectively. It is assumed that σ_H is perpendicular to the axis of the drift, while σ_h is parallel to the drift axis. The calculated in-situ stresses using equations (5 - 7), are shown in Table 3. It was assumed that there is no variability in the stresses with respect to the rock mass.

Table 3: In-situ stress component at 1000 m depth

Mining depth (m)	Unit weight (MN/m^3)	σ_v (MPa)	σ_H (MPa)	σ_h (MPa)
1000	0.027	27.0	50.7	34.8

PERFORMANCE FUNCTION FOR THE DRIFT

When a drift is excavated underground the original state of the rock mass surrounding the excavation is disturbed. This disturbance can be in the form of redistribution of stresses; creation of new fractures; closure and opening of existing fractures [46]. These changes have the potential of causing uncontrolled displacement or strain in the rock mass. The uncontrolled displacement could be in various forms such as ejection of material into an excavation caused by a rock burst, plastic deformation and squeezing of the rock mass, or wedge failure [47]. When the magnitude of the displacement exceeds a maximum tolerable limit then the excavation becomes unstable and cannot perform its functions. This tolerable limit is called the serviceability limit. Therefore, an underground excavation is regarded as being unstable if the magnitude of the displacement of the rock mass around an excavation exceeds the serviceable limit. The maximum displacement that a rock mass can withstand depends on the mechanical properties of the rock mass and the objective of the excavation. The deformation of the rock mass can also be expressed in terms of strain. Sakurai [48] proposed the concept of a critical strain limit which he used as a stability criterion for tunnels. Figure 3 shows the relationship between the critical strain and the uniaxial compressive strength (UCS) [49, 50]. The hazard warning level II in Figure 3 is the transition line from stable to unstable conditions. In this study, the hazard warning level II was used as the stability criterion for the drift. The equation for the hazard warning level II, estimated from Figure 3, can be expressed as

$$\varepsilon_{critical} = 10^{(-0.3601 Log UCS + 0.0702)} \tag{8}$$

where $\varepsilon_{critical}$ is the critical strain in percent. The value of the UCS of the rock mass can be estimated from the relationship proposed by [40] as:

$$UCS = \frac{2c\cos\phi}{1-\sin\phi} \tag{9}$$

where c is the cohesion and ϕ is the friction angle of the rock mass.

To determine the probability of instability of the drift a limit state function or performance function, $g(x)$, has to be defined as:

$$g(x) = R(x) - S(x) \tag{10}$$

where R and S are the critical strain and the strain around the drift due to the excavation, respectively. The strains in the roof and in the sidewalls of the drift were calculated from the displacements around the drift obtained from the numerical analyses. This will be discussed in Section 5. $R(x)$ and $S(x)$ are the probability density functions (PDFs) of the random variable x. For $g(x) > 0$ the drift is stable and the performance is satisfactory otherwise if $g(x) < 0$ the drift is unstable with unsatisfactory performance. The limit state boundary is therefore defined by $g(x) = 0$ and the probability of instability (Pf) can be defined as:

$$P_f = P[g(x) < 0] = \int_{g(x)<0} f(x) \tag{11}$$

where $f(x)$ is the joint PDF for the random variables, x. Another important characteristic for assessing the stability of geotechnical structures is the safety index or the reliability index (β). The reliability index can be defined as:

$$\beta = \frac{\mu_m}{\sigma_m} \tag{12}$$

where μ_m and σ_m are the mean and standard deviation of the PDF of $g(x)$, respectively. If the performance function can be assumed to follow a normal distribution then P_f can be defined as:

$$p_f = 1 - \phi(\beta) \tag{13}$$

where ϕ is the cumulative density function (CDF) of the standard normal variable.

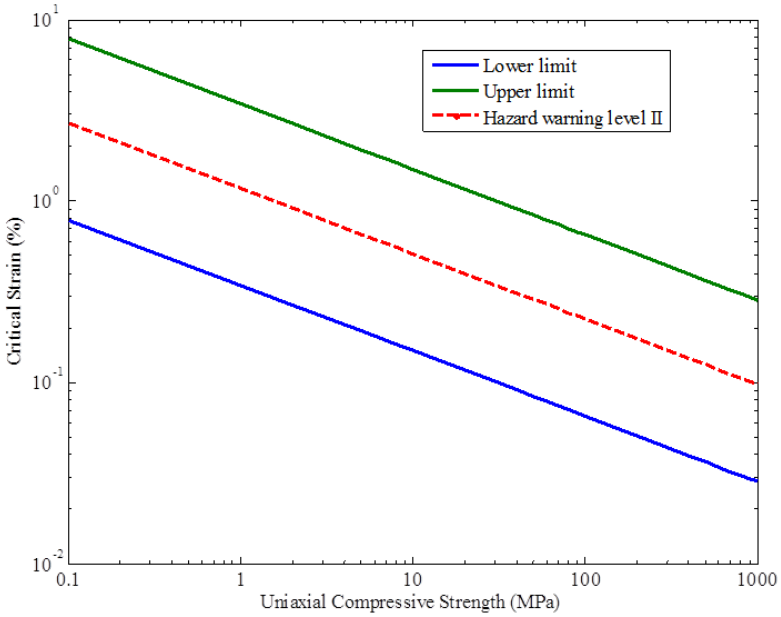

Figure 3: Sakurai's relationship between critical strain and UCS, also indicating hazard warning level II for assessing stability of tunnels (adapted from [49, 50])

NUMERICAL MODELLING

The numerical analyses of the drift were carried out using the explicit finite difference software FLAC [51]. FLAC has a built-in programming language called FISH which enables the user to define new variables and functions. This makes FLAC suitable for numerical analysis of complex rock mechanics problems. Two types of numerical analyses were conducted in this study: deterministic and probabilistic. In the deterministic models a single input value was used to represent each variable, while variability in the input values was considered in the probabilistic models.

The FLAC model size was chosen to be 77 m high and 77 m wide. These dimensions are large enough to eliminate boundary effects. The zone size of 0.25 x 0.25 m was used in the whole model to maintain the same zone size or mesh homogeneity. Roller boundary conditions were used for the model boundaries (see Figure 4).

The FLAC models were first brought to equilibrium with the stresses and boundary conditions applied before the excavation. Then the drift was excavated and the model cycled to equilibrium. The displacements normal to the boundary of the drift were tracked on the side walls, roof and the floor of the drift. The induced strains (ε) of the drift roof and sidewall were calculated from their respective radial displacements (U) from:

$$\varepsilon = \frac{U}{R} \tag{14}$$

where R is the equivalent radius of a circular opening with the same cross-sectional area (A) as the drift. R can be approximated from the relationship:

$$R = \sqrt{\frac{A}{\pi}} \tag{15}$$

Deterministic models

Mean values are often used as inputs deterministic analyses. However, extreme values such as worst case and best case values may also be considered. Experience and engineering judgment must be used when selecting these extreme values. For the deterministic models the mean values of the rock mass parameters were used as input parameters for the mean/expected case. The maximum values (mean + two standard deviations) and minimum values (mean – two standard deviations) of the input parameters were used for the best case and worst case, respectively. The mean values of the input parameters are summarized in Table 2. The in-situ stress components used for the models are those summarized in Table 3.

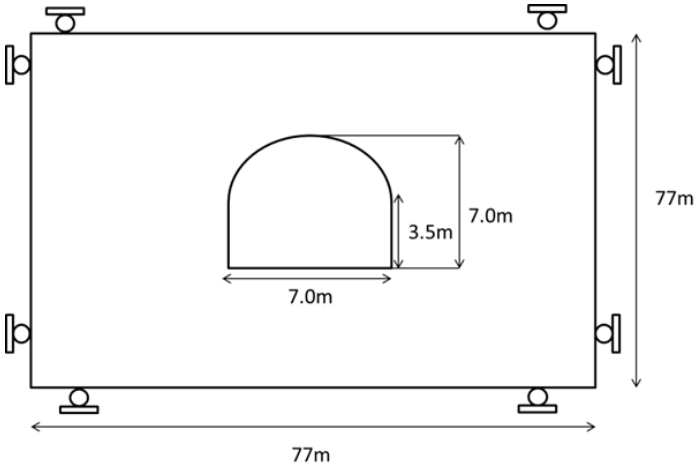

Figure 4: FLAC model size for the simulations

Deterministic model results

Induced strains around the drift (deterministic)

The induced strains around the drift due to the excavation were estimated from the displacements (perpendicular to the drift boundary) obtained in the left and the right sidewalls of the drift as explained previously. Since the induced strains of the left and right sidewalls of the drift are almost similar because of symmetry therefore only the results for the left sidewall were presented (Figure 5). The worst case showed the highest strain in the floor, roof and the sidewall of the drift when compared with the other cases. For the best and mean cases the strain in the sidewall was greater than that in the roof and the floor. However, when the rock mass becomes weaker as in the worst case the strain in the floor increased more significantly than in the sidewall and the roof of the drift. It can also be observed that the strain of the drift roof was very small compared with that of the floor and the sidewall for all cases. This may be due to the circular arch shape of the roof of the drift.

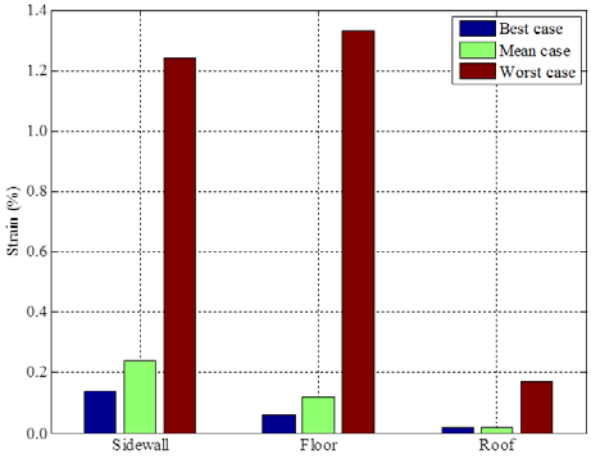

Figure 5: Strains around the drift for the best, mean and worst case models

Assessing the stability of the drift (Deterministic model)

In deterministic methods the factor of safety (FOS) is commonly used to assess the stability of geotechnical structures. FOS is the ratio of the capacity of the geotechnical structures to the applied load. A structure is deemed unstable when the FOS is less than 1 and it is stable when FOS is greater than 1. In this study the FOS was calculated as the ratio of the critical strain ($\varepsilon_{critical}$) defined by Equation 7 and the maximum calculated strain normal to the boundary around the drift boundary as explained in Section 5.1.

It can be seen from Table 4 that the sidewall and roof of the drift are stable for all cases except for the worst case in which the drift sidewalls are unstable. The strain of the sidewall for the worst case is greater than its corresponding critical strain (i.e. 0.57%). In the deterministic analysis, the calculated factor of safety does not consider the uncertainty in the input parameters hence the same value of FOS may be applied to different conditions with a varying degree of uncertainty. This approach eschews any information on the inherent risk associated with the design of the excavations.

Table 4: Estimated factor of safety for the sidewall and the roof of the drift for the three cases

Case	*UCS (MPa)*	$\varepsilon_{critical}$ (%)	Maximum strain, $\frac{U}{R}$ (%)		FOS	
			Sidewall	Roof	Sidewall	Roof
Best	71.54	0.25	0.14	0.02	1.79	12.5
Mean	37.19	0.31	0.24	0.04	1.29	7.75
Worst	7.59	0.57	1.24	0.17	0.46	3.35

Probabilistic models

In the probabilistic and deterministic analyses the same model geometry, in situ stresses, and boundary conditions were used. However, the uncertainties in the rock mass material properties were considered and also the simulation procedure adopted for each of the probabilistic methods were different from those of the deterministic analyses. In the following sections the input parameters and the simulation procedures for each of the probabilistic models are presented.

Point estimate method (PEM)

The Rosenblueth PEM was used in this study to avoid the problems associated with the modifications introduced by, for example, [18 – 21] (which was explained in Section 2.1). The four random variables are: the deformation modulus (E_m), the tensile strength (σ_t), the friction angle (ϕ), and the cohesion (c). Therefore, the total numbers of solution cases were 2^4 = 16. All of the four random variables were considered to be uncorrelated and normally distributed. The input parameters for all simulation cases for the rock mass are listed in Table 5. Each of the combinations of the input parameters for each case was used as input parameters in the FLAC models. Displacements of the sidewalls, roof and floor of the simulated drift were recorded for all sixteen cases and their statistical moments were determined. The displacements were recorded at the middle of the sidewall, roof and floor where the deformations are expected to be the highest. Induced strains were estimated from the

displacements as explained previously. In order to avoid negative values lognormal distributions were assumed for the results of the PEM models.

Table 5: Input parameters for the simulation cases for PEM

Case No	E_m (GPa)	ϕ (°)	c (MPa)	σ_t (MPa)
1	64.05	66.03	5.74	1.59
2	64.05	66.03	5.74	0.47
3	64.05	66.03	2.46	1.59
4	64.05	66.03	2.46	0.47
5	64.05	64.23	5.74	1.59
6	64.05	64.23	5.74	0.47
7	64.05	64.23	2.46	1.59
8	64.05	64.23	2.46	0.47
9	35.95	66.03	5.74	1.59
10	35.95	66.03	5.74	0.47
11	35.95	66.03	2.46	1.59
12	35.95	66.03	2.46	0.47
13	35.95	64.23	5.74	1.59
14	35.95	64.23	5.74	0.47
15	35.95	64.23	2.46	1.59
16	35.95	64.23	2.46	0.47

Response surface method (RSM)

For the RSM analysis, a full quadratic polynomial with cross terms was used to approximate the implicit relationship between the input parameters and the rock mass response around the excavated drift. The response surfaces were generated using the 2^n factorial design where n is the number of the random variables. Two evaluation points (upper and lower) were chosen for each of the random variables, i.e., the deformation modulus (E_m), the tensile strength (σ_t), the friction angle (ϕ), and the cohesion (c). The upper and lower evaluation points were defined as $x_u = \mu + k\sigma$ and $x_l = \mu - k\sigma$, respectively, where μ is the mean and σ is the standard deviation. The evaluation point values are based on the assumption that the input parameters are normally distributed. The value of the parameter k was chosen to be 1. In later analyses it was increased to 2 to study the effect of the evaluation points on the RSM results. Sixteen different combinations of the input parameters were generated similarly to that of the PEM. Using the same modeling procedure as that of the PEM analysis (Section 4.2.1) 16 different strain values of the middle of the sidewall, roof and floor of the simulated drift were estimated from their corresponding displacements. These values were used to obtain the response surface equations for the strains of the drift boundaries. The normal probability plots (not shown) for the regression model for the equations were approximately straight lines with the value of R^2 ranging from 0.94 to 0.98. The R^2 is the coefficient of determination and indicates the accuracy of the fitted regression model. The closer the R^2 is to 1, the more accurate the regression model. The statistical moment of the strains of the drift boundary were computed from Monte Carlos Simulations of 10^5 trials using the response equations. The program @RISK was used for this purpose.

Artificial neural network

The ANN was used to approximate the relationship between the response of the rock mass surrounding the excavated drift (i.e. strain) and the random input parameters. The random input parameters were the deformation modulus (E_m), the tensile strength (σ_t), the friction angle (ϕ), and the cohesion (c).

The training datasets for establishing the ANN model were selected using the uniform design method proposed by [52, 53]. The Uniform design method is capable of providing samples with high representativeness and it can reduce the number of experimental runs when there are many factors and multiple levels [54 – 56]. Twenty-six (26) datasets were used as training data for the ANN model. Twenty-six (26) combinations of the random values of the input parameters were generated by considering uniformly spaced twenty-six sampling points for each random value within the range of ± 1 standard deviation from their respective means. The range of ± 2 standard deviations of the respective mean of the random input parameters were also considered for comparison. The details of how the uniform design method was used to design the ANN model training datasets is presented in Appendix A. The twenty-six combinations of the input parameters were used to generate corresponding twenty-six responses in terms of strains around the drift using the FLAC software in a similar way as that of the aforementioned models/analyses. Both input parameters and the responses were normalized or scaled to be in the range of ±1 because the ANN algorithm (especially the back-propagation algorithm) works best when the training data is scaled or normalized [30].

The architecture of the ANN was designed using the multilayer perceptron (MLP) feed-forward neural network which is commonly used in geotechnical engineering analyses [32, 57]. For the development of the network, a commercial software package MATLAB [58] was used to simulate the ANN operations. The network has one input layer, one output layer and one hidden layer. The input layer has four neurons and the output layer also has four neurons. The number of neurons in the hidden layer was chosen to be 5 as this gave the best result. The best configuration was achieved in this work by using the linear transfer function (purelin) in the output layer and the hyperbolic tangent sigmoid (tansig) transfer function in the hidden layer. The network was trained with the Levenberg-Marquardt back-propagation algorithm (trainlm) using the 26 normalized datasets. During the training process the weights and biases were iteratively adjusted to reduce the mean squared error (MSE) between the ANN predicted values and targeted values. A sub-set of the training dataset was randomly selected for the validation and testing of the ANN model. The accuracy of the ANN model was determined using the coefficient of determination (R^2). The R^2 was greater than 0.9 for the model training, validation and testing of the two cases (i.e. two sampling points) considered for the ANN simulations.

Having trained the models accurately, the optimal weights and biases were extracted from the network models and used to develop the mathematical expressions relating the input parameters and the rock mass responses (i.e. strains) around the excavated drift. The statistical moments and PDFs for the strains around the drift were determined from 10^5 MCS trials using the mathematical expressions for the strains obtained for the ANN model. The MCS trials were performed using the excel-ad-in program @RISK.

Monte Carlo simulation model

The Monte Carlo simulation (MCS) method was used to incorporate both variability and heterogeneities of the input parameters into the FLAC model for the analysis of the drift stability. The model geometry and the boundary conditions were the same as that of the deterministic models as well as the other probabilistic models. The random material properties and their statistical moments

used for the MCS model are listed in Table 2. These material properties were randomly assigned from their PDFs to the zones of the FLAC model using the FLAC inbuilt FISH functions. Figure 6 shows an example of the random distribution of the shear modulus in one of the models in the MCS simulations. The correlation between the input parameters and the spatial correlation of the heterogeneities are not considered in this model. Ten thousand (10^4) simulations of the MCS model were run which generated random distributions of displacements of the sidewalls, roof and floor of the simulated drift. The induced strains were estimated from the displacements as discussed previously. Figure 7 shows the best fit (lognormal) PDF for the induced strain of the drift sidewall, roof and floor obtained from the MCS simulations. The statistical moments for the induced strains were obtained from the PDFs.

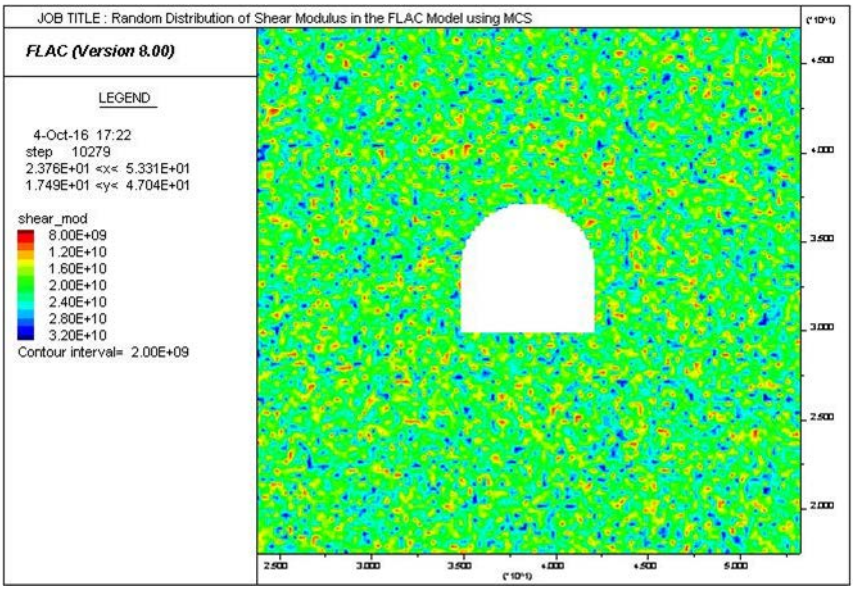

Figure 6: Random distribution of shear modulus in a MCS model

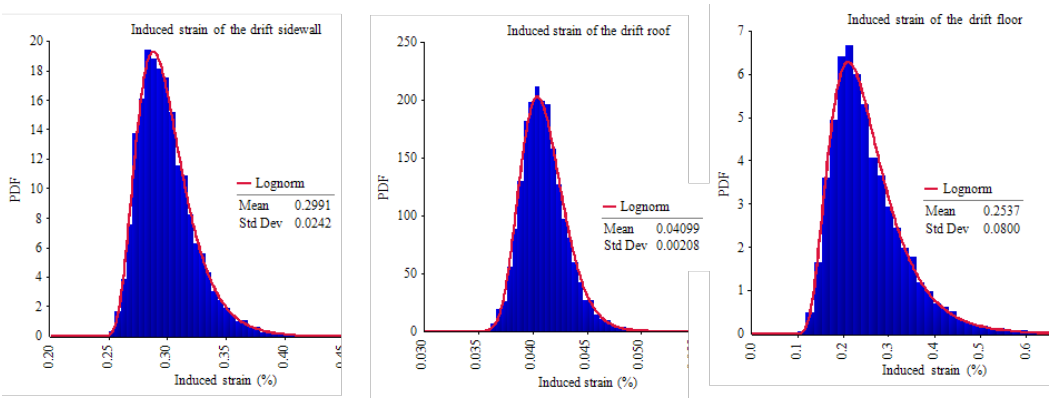

Figure 7: PDFs of induced strain of the drift sidewall, roof and floor for MCS Model

Strength classification method model

The Strength Classification Method (SCM) also considers variability and heterogeneity in the rock mass properties. This method is used since it reduces the time needed to run a single simulation, though the total number of simulations required may be the same as that of the MCS. The random input parameters, the deformation modulus (E_m), the tensile strength (σ_t), the friction angle (ϕ), and the cohesion (c), were all treated as normally distributed as shown in Table 2. Each PDF of the random input parameters was partitioned into three strength classes: the high, medium and low strength based on their mean values (μ) and standard deviations (σ). The interval for each class and the area (or probability) covered within each interval are presented in Figure 7. It should be noted that the total area covered by the interval $\mu \pm 3\sigma$ is 0.997 for a normal distribution PDF. However, in this study for simplicity it was approximated to 1. The middle value of each interval was used to represent each strength class. For instance, the middle value of the input parameter for high strength class corresponds to $\mu+2\sigma$.

To implement this in the FLAC model, the number of zones for each strength class in the entire model was calculated based on their specified probabilities (or area covered). FISH functions were written to randomly select the zones and assign accordingly the corresponding material properties. The location of each variable was randomly varied between each realization of the numerical simulation. The model geometry and boundary conditions were the same as those of the deterministic model and the other probabilistic models.

Similar to the MCS model 10^4 simulations were run using this method and this generated 10^4 random distributions of the displacements around the drift similar to the MCS model. The induced strains were also estimated from the displacements. The best fit (lognormal) PDFs for the induced strains of the drift sidewall, roof and floor obtained from the SCM simulations are shown in Figure 8. The statistical moments for the induced strains were also obtained from the PDFs. The correlation between the input parameters and the spatial correlation of the heterogeneities were not considered in this model.

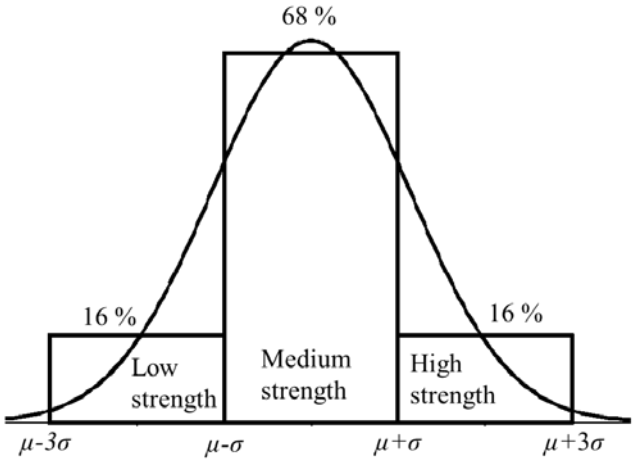

Figure 7: Interval for each class of the random input parameters and their corresponding probabilities

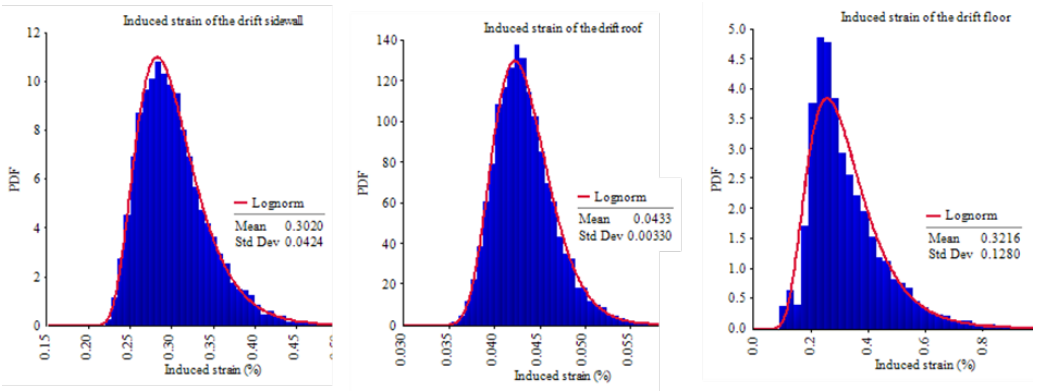

Figure 8: Assessed PDFs of induced strain of the drift sidewall, roof and floor for SCM Model

Probabilistic model results

Two different models were considered for RSM based on the evaluation points and ANN sampling range. They are referred to as RSM_1, RSM_2, ANN_1 and ANN_2, respectively. The evaluation points for the input parameters for the RSM_1 model were selected at μ-σ and μ+σ while the evaluation points for the input parameters for the RSM_2 were selected to be μ-2σ and μ+2σ. The sampling range for the input parameters for the ANN_1 and the ANN_2 training datasets were μ-σ to μ+σ and μ-2σ to μ+2σ, respectively. The μ in the mean and σ is the standard deviation for the input parameters.

Induced Strain around the drift (Probabilistic)

The induced strains estimated from the displacements at the boundary of the excavated drift which were obtained from the different probabilistic methods are shown in Tables 6, 7 and 8. The maximum and minimum values for the strain were taken at 95% confidence interval. The results for all the models were assumed to follow a lognormal distribution.

The strains of both sidewalls of the drift obtained from the PEM, RSM and ANN models were similar because of the assumption of homogeneity of the material properties and the symmetry of the models. Therefore only the strain of the left sidewall is presented for the PEM, RSM and ANN models. For comparison purposes the strains of the left sidewall were also presented for both the MCS and the SCM models. The mean values of the strains of the sidewall and roof of the drift as presented in Tables 6, 7 and 8 are reasonably similar for the different methods used. However, a noticeable exception is evident for the RSM_2 model. The RSM_2 model strains are almost twice those of the other models, which could be due to the evaluation points of the input parameters used to generate the response surface equations. It is observed that the mean values of the strain for the drift floor obtained from MCS and SCM models were greater than those obtained from other probabilistic models (except RSM_2) which shows that the heterogeneity models shows more deformation on the drift floor than other models. The coefficient of variation (COV) of the strains around the drift (except drift floor) calculated using the MCS and the SCM is smaller when compared to those obtained from the other methods considered.

Table 6: Induced strain of the drift sidewall

Method	Mean (%)	COV (%)	Maximum (%)	Minimum (%)
PEM	0.27	31.40	0.47	0.14
RSM_1	0.27	27.04	0.43	0.14
RSM_2	0.52	30.49	0.87	0.25
ANN_1	0.27	31.73	0.44	0.10
ANN_2	0.27	46.96	0.61	0.16
MCS	0.30	8.08	0.35	0.25
SCM	0.30	14.04	0.39	0.23

Table 7: Induced strain of the drift roof

Method	Mean (%)	COV (%)	Maximum (%)	Minimum (%)
PEM	0.04	30.73	0.07	0.02
RSM_1	0.04	25.84	0.06	0.02
RSM_2	0.08	33.78	0.15	0.04
ANN_1	0.04	25.79	0.06	0.02
ANN_2	0.04	43.33	0.09	0.03
MCS	0.04	5.10	0.05	0.04
SCM	0.04	7.67	0.05	0.04

Table 8: Induced strain of the drift floor

Method	Mean (%)	COV (%)	Maximum (%)	Minimum (%)
PEM	0.15	43.66	0.32	0.06
RSM_1	0.15	37.45	0.28	0.06
RSM_2	0.43	38.20	0.81	0.17
ANN_1	0.15	31.96	0.26	0.04
ANN_2	0.16	47.29	0.31	0.01
MCS	0.25	31.42	0.44	0.13
SCM	0.32	39.80	0.64	0.15

Assessing the drift stability using performance function

The stability of the drift was assessed by determining the probability of instability (p_f) and its reliability index (β) for the drift. The performance functions (Equation 10) were developed using the critical strain equation (Equation 8) and the mathematical expressions for strains obtained from the RSM_1, RSM_2, ANN_1 and ANN_2 models. For the PEM, MCS and SCM models the statistical parameters and the probability density functions of the strains obtained from the models were used together with the critical strain equation to develop their performance functions. Monte Carlo simulations with 10^5 trials were performed on the performance functions using the program @RISK. The mean values and standard deviations of the performance functions were estimated and the reliability indices (β) (i.e. mean values divided by standard deviation of the performance function) were determined. Also the probabilities of instability were calculated from the reliability indices. When using this approach to estimate the probability of instability (p_f), the performance function was assumed to be normally distributed. The performance function may not be normally distributed in all cases hence the approach should be used carefully. Table 9 shows the reliability indices and instability probabilities of the drift obtained from the different probabilistic models. All the probabilistic model results show that the roof of the drift is expected to be stable (Table 9). The RSM_2 model gives the highest probability of instability for the drift sidewall compared to the other models while the ANN_2 model gives the lowest probability of instability for the drift sidewall. In Table 9 the reliability index for the RSM_2 model has a negative value because the mean value of the performance function (μ_m) for the model is less than zero. Negative values of β occur when (p_f) is greater than 50%.

Table 9: Reliability indices and probability of instability of the drift with respect to different probabilistic methods

Method	Sidewall		Roof	
	$\beta = \frac{\mu_m}{\sigma_m}$	$p_f = 1-\phi(\beta)(\%)$	$\beta = \frac{\mu_m}{\sigma_m}$	$p_f = 1-\phi(\beta)(\%)$
PEM	0.60	27.43	5.30	5.79×10^{-06}
RSM_1	0.65	25.78	5.53	1.60×10^{-06}
RSM_2	-1.38	91.62	5.33	4.91×10^{-06}
ANN_1	0.58	28.10	5.27	6.82×10^{-06}
ANN_2	0.66	25.46	5.70	5.99×10^{-07}
MCS	0.56	28.64	5.44	2.66×10^{-06}
SCM	0.45	32.64	5.40	3.33×10^{-06}

DISCUSSION

Comparison between deterministic and probabilistic models

The sidewall strains obtained from the three cases analyzed with the deterministic method were compared with the sidewall strains obtained from the probabilistic models as shown in Figure 9. The deterministic best and mean case results show good agreement with the minimum and mean values of the probabilistic models for all the methods except the RSM_2. The worst case model shows a large difference from the maximum values of the probabilistic models. Therefore using the worst case model to cater for the inherent variability in the input parameters will not only make the inherent risk in the design obscured but could result in a very conservative design. The best and the mean cases of the deterministic model may give similar results as those representing the minimum and mean values of the probabilistic models but they do not provide any information on the inherent risk in the analysis. The best case is seldom used in geotechnical design as it could lead to an overestimation of strength parameters of the rock mass.

The factor of safety (FOS) estimated from the deterministic models (Table 4) when compared with the probability of instability obtained from the probabilistic models (Table 9) shows that the drift sidewall would remain stable except for the worst case whereas the probabilistic model results indicate that there would be at least a 20% probability of instability for the drift sidewalls. The performance level of a system whose probability of failure/instability is greater than 16% is hazardous according to the rating of the US Army Corps of Engineers [59]. Although it may be argued that the minimum allowable FOS could be increased (i.e. > 1) to compensate for the inherent variability in the input parameters it could still lead to a very conservative design. In addition, information on the likelihood of occurrence of instability of the drift would become obscured.

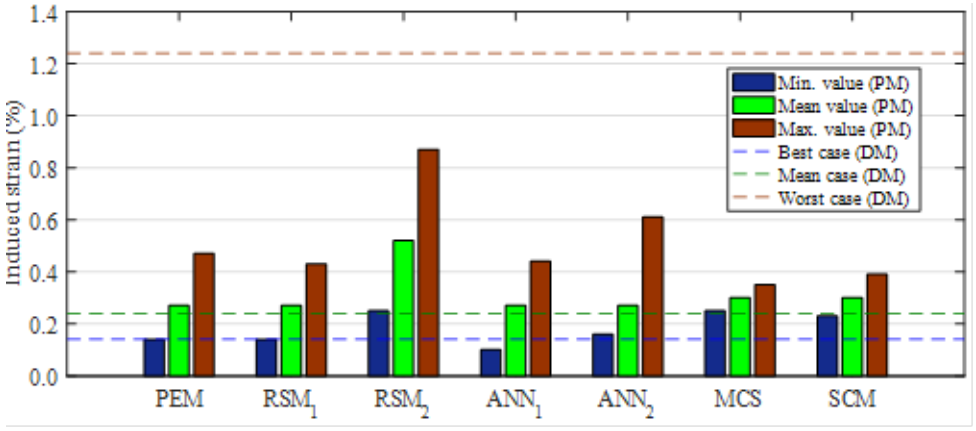

Figure 9: Comparison between deterministic and probabilistic models (PM = Probabilistic models and DM = Deterministic models)

Comparison of the probabilistic models

To compare the probabilistic methods used in this study the following factors were considered: (1) the accuracy of the results (2) the computation time and simplicity of each model and (3) the effect of the variability of the rock mass on the drift failure pattern.

Accuracy of the results of the models

When the number of simulations is large enough to achieve desired accuracy direct Monte Carlo simulations provide more accurate results than any other probabilistic method. In this study the results obtained from the 10^4 iterations of the MCS model could be assumed to provide the "exact" probability of failure for the drift sidewall and therefore used as the standard for the comparison. Direct MCS of 10^4 iterations have also been used for reliability analyses [60].

The relative error in the probability of instability (p_f) estimated from each model to that of the MCS model was calculated using the following relation:

$$\text{Relative error} = \frac{p_{f(\text{model})} - p_{f(MCS)}}{p_{f(MCS)}} \times 100 \tag{16}$$

where $p_{f(\text{model})}$ is the probability of instability estimated from each model and $p_{f(MCS)}$ is the probability of instability estimated from the MCS model. The probability of instability for the sidewall of the drift was used for the comparison of the accuracy of the results. Table 10 shows that ANN_1 model has the lowest relative error, followed by PEM model. This indicates that within the context of this study ANN_1 and PEM could have almost the same results as that of the MCS model. The SCM model showed higher relative error than other models except RSM_2 though it is expected that SCM model results will be closer to MCS model than other models being heterogeneous model as MCS. This could be due to the three partitions of the PDFs of the input parameters used which could leads to higher COV.

The RSM_2 model results have the highest relative error. The significant difference in the strain between the RSM_2 model and the other models could be attributed to the evaluation points of the input parameters used for generating the response surface equations. Depending on the magnitude of the variance of the random input parameters, when the evaluation points for the input parameters are located too far from the mean values sudden change in the behavior of the model (e.g. elastic to plastic) could occur. In such a situation the combinations of the inputs selected at the lower evaluation point could produce high magnitude of model response (e.g. strain) and those selected at the upper sampling point could produce low magnitude of the response. This may lead to higher mean value and variance of the results of all the simulations. In geotechnical problems ±1 standard deviation around the mean value is often used as the evaluation points for the RSM models e.g. [12, 61]. It has also been reported that evaluation points closer to the mean values can improve the fit of the RSM [61, 62]. Wong [63] also observed that when the sampling points are far away from the mean value the RSM becomes less accurate except in cases when more points are employed.

Contrary to the results of the RSM_2 model, the ANN_2 model has small relative error despite the fact that the range of the sampling points for ANN_2 training datasets was μ-2σ to μ+2σ. The explanation for this could be the uniform design sampling method used for selecting the samples for the training of the ANN model. This ensures a uniform distribution of the sampling points (i.e. 26 points) within ± 2 standard deviations from the mean value leading to high representation of the samples in the ANN training. The twenty-six simulations using the combinations of the 26 different uniformly spaced sampling points of the input material could have prevented a sudden change in the behavior of the numerical model. Furthermore, the back-propagation procedure of the training and testing of the ANN model could give the ANN model more predictive power than the RSM. The relative error of the ANN_2 (11.1%) shows that the range of the sampling points used for the ANN training datasets does not have much effect on the results of the ANN model, as observed in RSM_2, especially when the training datasets were selected using the uniform design method.

Table 10: Relative error estimated from the models compared with that of the ANN_1 model

Model	Relative error (%)
PEM	-4.22
RSM_1	-9.99
RSM_2	219.9
ANN_1	-1.89
ANN_2	-11.10
MCS	-
SCM	-13.97

Computation time and simplicity of model

The total execution time required for the simulations of the different probabilistic models used in this study is summarized in Table 11. The simulations were run on a computer with a 2.80 Ghz Intel Core i7 930 of 12GB RAM with Windows 7 (64-bit) as the operating system. The computational time for the SCM model was almost 20% less than that for the MCS model. This may be because the SCM model has 3 different sets of material properties randomly distributed within the model. This means that the solution scheme of the SCM model in the FLAC requires fewer steps to reach equilibrium than the steps required for the MCS model to reach equilibrium. The MCS and the SCM models give similar results as the SCM model may replace the MCS model as the time required for the computation is shorter.

The computation time for all the models as presented in Table 11 excluded the time for the preparation of the input parameters, processing, and analyses of the results which involve the use of different software in the case of the ANN and the RSM models. A simpler probabilistic model reduces the time and efforts required for the preparation of input parameters, processing, and analyses of the results. This may be desirable in some practical applications. The PEM method is the simplest of the methods studied as less time and effort is required for the preparation of input parameters for the numerical simulation and the processing of results. The preparation of input parameters for the RSM model and the PEM model are the same. However, the processing of the RSM model results needs statistical software to generate the response surface equations. When the number of random variables used as input parameters is greater than 4 or 5 the number of simulations required for the Rosenblueth PEM and the full factorial designed RSM increases exponentially and this increases the computation time.

The number of simulations required for training the ANN model is more than the number of simulations required for generating the response equations and number of simulations for the Rosenblueth PEM. For large number of variables, the ANN would have an advantage over the PEM and the RSM in terms of the number of simulations required, especially when uniform design method is used to select the training datasets for the ANN model.

The MCS and the SCM models are very simple to implement, though FISH codes are required for the implementation in the FLAC model. The results of the MCS and the SCM can be quite

accurate if enough simulations are performed. The required number of simulations to achieve such accuracy could be in the thousands hence consuming a lot of time.

Table 11: Computation time for different probabilistic models

Probabilistic method	Total computation time
PEM (16 simulations)	44 minutes
RSM (16 simulations)	44 minutes
ANN (26 simulations)	60 minutes
MCS (10000 simulations)	33610 minutes
SCM (10000 simulations)	27250 minutes

Effect of rock mass variability on the drift failure pattern

Figure 10 shows the shear strain plots for some of the cases analyzed with the PEM model. These were used to represent the homogeneous models since the RSM and the ANN models show similar behavior. The shear strain plots for the MCS model are shown in Figure 11. The shear strain plots of the MCS model are similar to those of the SCM model. The shear strain concentration shown in the plots depends on the chosen contour interval. For the purpose of comparison of the PEM and the SCM model results a contour interval value of 0.2% was used for the shear strain plots. Based on the chosen contour interval for the shear strain plots, case 1 of the PEM model shows no shear deformation (i.e. the shear strains around the drift are less than 0.2%) while shear strain concentrations are visible only in the sidewall of the drift in case 9 and in the sidewall, floor and roof of the drift in case 16 (Figure 11). The input parameters for the cases have been presented in Table 5. This shows that the shear strain concentration at the drift boundary obtained from the analyses using the PEM, the RSM and the ANN models depends on the combination of the input parameters used for each simulation. Hence they may result in different failure patterns than those obtained from the MCS and the SCM models. In contrast to the results from the homogeneous models, all the simulations of the MCS or the SCM model show shear strain concentrations (i.e. the shear strains around the drift are greater than 0.2%) in the sidewall and in the floor of the drift as shown in Figure 11. However, to use this kind of shear strain plot to discuss the stability of the drift, the critical shear strain has to be assessed (estimated) and the plot contour interval chosen so only the concentrations which are critical are visualized.

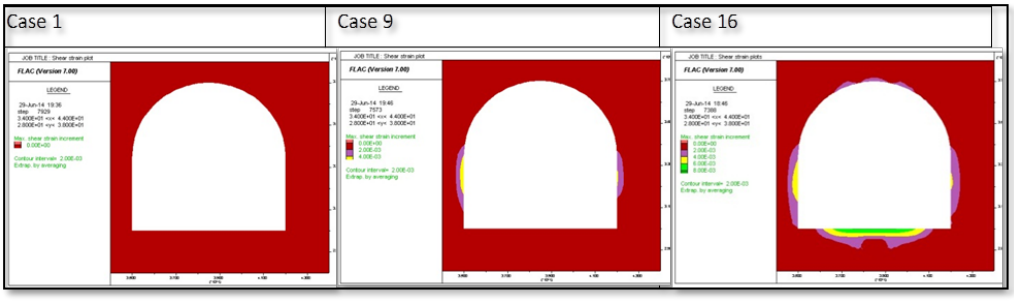

Figure 10: Shear strain plot for cases 1, 9 and 16 of the PEM model

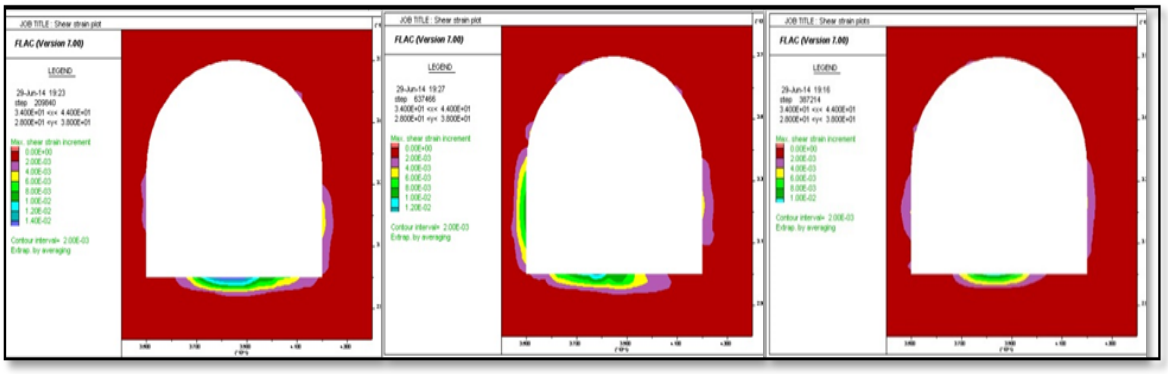

Figure 11: Some examples of shear strain plots taken from 104 simulations of the MCS model

CONCLUSIONS

Uncertainty and variability are peculiar to geotechnical materials such as rock masses. For realistic analyses of the stability of excavations within a rock mass the variability and uncertainty in the properties of the rock mass must be adequately considered using probabilistic methods. Since there are many probabilistic methods based on different theories and assumptions selecting the appropriate one is desirable. In this study five different probabilistic methods were incorporated with FLAC to analyze the stability of a drift excavated within a rock mass with varying material properties. The probabilistic methods considered were the PEM, the RSM, the ANN, the MCS and the SCM. The potentials and the limitations of each method were discussed. The importance of considering the variability in the rock mass properties in the stability analyses of underground excavations was also discussed by comparing the deterministic model results with that of the probabilistic models. Some of the major conclusions are summarized below:

(i) The use of the best and worst cases in a deterministic stability analysis of an underground excavation has not reflected the risk inherent in the analysis. The best case is seldom used in design as it could overestimate the strength of the rock mass while the worst case could results in a very conservative design.

(ii) The ANN requires more computation time and effort than the PEM and the RSM when a uniform design approach is used to design the training data. However, it is more accurate than the PEM and the RSM. The ANN is less sensitive to the range of sampling points used for the ANN training datasets. The accuracy of the result of the RSM can be affected when the evaluation points of its input parameters are far away from the mean values.

(iii) The PEM is the simplest of the probabilistic methods considered in this study and it required the shortest computation time. The PEM results were very similar to that of the MCS model. Therefore, when few random input variables are used in the analysis (e.g. $\leq$ 4) the PEM should be used instead of the ANN or RSM.

(iv) The PEM, the RSM and the ANN are not designed to qualitatively describe the failure pattern of the excavated drift because each of the combinations of the input parameters used for each simulation leads to a different failure pattern or in some cases no failure. In

the case when the heterogeneity of the rock mass is paramount in the analysis the MCS or the SCM could be used.

(v) Both the MCS and the SCM are very simple to implement in the numerical model, however, they required a large number of simulations to obtain a certain level of accuracy. The SCM required less computation time compared with the MCS hence is an alternative to MCS since both showed similar results.

(vi) This study has not covered all the existing probabilistic methods: however, the results of this study could assist in the selection of the appropriate probabilistic method, within those covered in this study, for a specific objective while considering the accuracy, computation time and simplicity.

ACKNOWLEDGEMENT

The authors express their thanks to the Centre of Advanced Mining and Metallurgy (CAMM) at the Luleå University of Technology, Luleå, Sweden for financial support.

Appendix A. Application of the uniform design method for selecting training data for the ANN model

A table of uniform design (UD) is denoted U_n (q^t) where n is the number of the experimental runs, q is the number of levels of each factor and t is the number of the factors [64]. The procedure used in preparing the training datasets for the ANN model using the UD method is explained with Table A.1. The number of factors was 4 (i.e. input variables) with 26 levels for each factor. The sampling points for each random variable which ranged between ± 1 standard deviation from the mean value was used here to explain the procedure. The interval [-1, 1] was divided into 25 sub-intervals with equal length. The 26 end points of these sub-intervals are denoted k_i (i = 1, 2, 3……, 26). Since the number of factors is 4 and each factor having 26 levels, the U_{26} (26^4) UD table was used to design the input training data. The input training data (rows denoted case # 1 - 26) was obtained as follows: The columns *I*, *II*, *III*, and *IV* in the UD table (Table A1) correspond to E_m, c, σ_t and ϕ, respectively. In order to obtain, for instance, the value of E_m for case # 1 the index i can be found in column *I*, i.e., i = 18. The value of k_{18} = 0.36 is obtained from Table A.2. Deformation modulus, E_m, is then calculated using the relation $\mu_{E_m} + k_{18}\sigma_{E_m}$ where μ_{E_m} and σ_{E_m} are the mean and standard deviation of E_m, respectively, and are found in Table 2: μ_{E_m} = 50 GPa and σ_{E_m} = 14.05 GPa. Hence, deformation modulus, E_m , for case # 1 is equal to 55.06 GPa (see Table A.1). The values of all the four input parameters for all the 26 cases were determined in this manner using the UD table.

Table A.1: UD table and ANN input training data

Case #	i = UD table (U_{26} (26^4)				E_m (GPa)	c (MPa)	σ_t (MPa)	ϕ (°)
	I	*II*	*III*	*IV*				
1	18	11	18	1	55.06	3.77	1.21	64.23
2	11	4	4	3	47.19	2.85	0.64	64.37
3	7	10	10	14	42.69	3.64	0.89	65.17
4	20	2	12	9	57.31	2.59	0.97	64.81
5	19	26	15	16	56.18	5.74	1.09	65.31
6	2	3	8	22	37.07	2.72	0.81	65.74
7	8	25	5	10	43.82	5.61	0.68	64.88
8	21	16	24	23	58.43	4.43	1.46	65.81
9	4	17	2	17	39.32	4.56	0.56	65.38
10	14	7	14	26	50.56	3.25	1.05	66.03
11	26	5	17	18	64.05	2.98	1.17	65.45
12	22	8	1	12	59.55	3.38	0.52	65.02
13	12	18	11	19	48.31	4.69	0.93	65.53
14	6	24	19	25	41.57	5.48	1.25	65.96
15	15	14	7	5	51.69	4.17	0.76	64.52
16	13	22	26	13	49.44	5.22	1.54	65.09
17	3	20	13	2	38.20	4.95	1.01	64.30
18	5	6	25	6	40.45	3.12	1.50	64.59
19	16	1	21	15	52.81	2.46	1.34	65.24
20	24	12	6	24	61.80	3.90	0.72	65.89
21	10	15	16	8	46.07	4.30	1.13	64.73
22	25	23	9	7	62.93	5.35	0.85	64.66
23	23	19	22	4	60.68	4.82	1.38	64.45
24	9	9	23	20	44.94	3.51	1.42	5.60
25	1	13	20	11	35.95	4.03	1.30	64.95
26	17	21	3	21	53.93	5.08	0.60	65.67

Table A.2: Division of the interval into sub-intervals and end points of each sub-interval

i	k_i
1	-1.00
2	-0.92
3	-0.84
4	-0.76
5	-0.68
6	-0.60
7	-0.52
8	-0.44
9	-0.36
10	-0.28
11	-0.20
12	-0.12
13	-0.04
14	0.04
15	0.12
16	0.20
17	0.28
18	0.36
19	0.44
20	0.52
21	0.60
22	0.68
23	0.76
24	0.84
25	0.92
26	1.00

REFERENCES

1. Martin, C.D., Kaiser, P.K. and McCreath, D.R. (1999) Hoek-Brown parameters for predicting the depth of brittle failure around tunnels. Can. Geotech. Journal, 36 (1), pp. 136-151.
2. Idris, M. A., Basarir, H., Nordlund, E., and Wettainen, T. (2013) The probabilistic estimation of rock masses properties in Malmberget mine, Sweden. Electronic Journal of Geotechnical Engineering, (18. B) pp. 269-287.
3. Phoon, K.K. and Kulhawy, F.H. (1999) Characterization of geotechnical variability. Can. Geotech. Journal, 36 (4), pp. 612-624.

4. Valley B, Kaiser P.K, Duff, D. (2010) Consideration of uncertainty in modelling the behaviour of underground excavations. In: Proceeding of 5th International seminar on Deep and High Stress Mining, Santiago, pp. 423-435.
5. Chen, G., Jia, Z., and Ke, J. (1997) Probabilistic analysis of underground excavation stability. Int. J. Rock Mech. Min. Sci. 34 (3-4), pp. 51e1-51e16.
6. Hoek, E. (1998) Reliability of Hoek-Brown estimates of rock mass properties and their impact on design. Int. J. Rock Mech. Min. Sci. 35, pp. 63-68.
7. Pathak, S. and Nilsen, B. (2004) Probabilistic rock slope stability analysis for Himalayan condition. Bull Eng. Gel. Environ 63 pp. 25–32.
8. Mollon, G., Dias, D. and Soubra, A.H. (2009) Probabilistic analysis of circular tunnels in homogeneous soil using response surface methodology. J. Geotech. Geoenviron. 135 (9) pp. 1314-1325.
9. Cai, M. (2011) Rock mass characterization and rock property variability considerations for tunnel and cavern design. Rock Mech. Rock Eng. 44 (4) pp. 379-399.
10. Idris, M.A., Saiang, D. and Nordlund, E. (2011) Probabilistic analysis of open stope stability using numerical modelling, Int. J. of Mining and Mineral Engineering. 3, pp. 194-219.
11. Goh, A.T.C. and Zhang, W. (2012) Reliability assessment of stability of underground rock caverns. Int. J. Rock Mech. Min. Sci. 55, pp. 157- 163.
12. Lü, Q. and Low, B.K. (2011) Probabilistic analysis of underground rock excavations using response surface and SORM. Computers and Geotechnics. 38 (8) pp. 1008-1021.
13. Langford, J.C. and Diederichs, M.S. (2013) Reliability based approach to tunnel lining design using a modified point estimate method. Int. J. Rock Mech. Min. Sci. 60, pp. 263-276.
14. Park, D., Kim, H.M., Ryu, D.W., Song, W.K. and Sunwoo, C. (2012) Application of a point estimate method to the probabilistic limit-state design of underground structures. Int. J. Rock Mech. Min. Sci. 51, pp. 97-104.
15. Rosenblueth, E. (1975) Point estimates for probability moments. Proc Nat Acad Sci USA. 72(10), pp. 3812-3814.
16. Rosenblueth, E. (1981) Two-point estimates in probabilities. J Appl Math Model 5 (5) pp. 329-335.
17. Christian, J.T. and Baecher, G.B. (1999) Point estimate method as numerical quadrature. J. Geotech. Geoenviron. 125 (9) pp. 779-786.
18. Harr, M.E. (1989) Probabilistic estimates for multivariate analyses. Applied Mathematical Modelling, 13 pp. 313 -318
19. Li, K.S. (1992) Point estimate method for calculating statistical moments. Journal of Engineering Mechanics, 118 (7), pp. 1506-1511.
20. Chang, C.H., Tung, Y.K., and Yang, J.C. (1995) Evaluation of probability point estimate methods. Applied Mathematical Modelling, 19(2), pp. 95-105.
21. Hong, P. (1998) An efficient point estimate method for probabilistic analysis. Reliability Engineering and System Safety 59(3), pp. 261-267.

22. Christian, J.T. and Baecher, G.B. (2002) The point estimate method with large numbers of variables. International Journal for Numerical and Analytical Methods in Geomechanics. 26, pp. 1515-1529.

23. Abdellah, W., Mitri, H.S., Thibodeau, D., and Moreau-Verlaan, L (2014) Geotechnical risk assessement of mine development intersections with respect to mining sequence. Geotech Geol Eng., 32, pp.657-671.

24. Lü, Q., Chan, C.L., and Low, B.K. (2012) Probabilistic evaluation of ground-support interaction for deep rock excavation using artificial neural network and uniform design. Tunnelling and Underground Space Technology, 32, pp. 1-8.

25. Lee, C., and Sterling, R. (1992) Identifying probable failure modes for underground openings using neural a network. Int. J. Rock Mech Min Sci Geomech Abstr. 29, pp. 49-67.

26. Moon, H.K., Na, S.M., and Lee, C.W. (1995) Artificial neural network integrated with expert system for preliminary design of tunnels and slopes. In: Proceedings of the 8th International congress on rock mechanics, pp. 901-905, Balkema.

27. Yoo, C., and Kim, J.M. (2007) Tunneling performance prediction using integrated GIS and neural network, Computer and Geotechnics, 34, pp. 19-30.

28. Mahdevari, S., and Torabi, S.R. (2012) Prediction of tunnel convergence using artificial neural networks. Tunnelling and Underground Space Technology, 28, pp. 218-228.

29. Idris, M.A., Saiang, D., and Nordlund, E. (2015). Stochastic assessment of pillar stability at Laisvall mine using Artificial Neural Network. Tunnelling and Underground Space technology, 49, pp. 307-319.

30. Beale, M.H., Hagan, M.T., and Demuth, H.B. (2012) Neural Network Toolbox User's Guide. The MathWorks Inc. Natick, MA.

31. Hornik, K., Stinchcombe, M., and White, H. (1989) Multilayer feedforward networks are universal approximators. Neural Networks. 2, pp. 359-366.

32. Sahin, M.A., Jaksa, M.B. and Maier, H.R. (2008) State of the Art of Artificial Neural Networks in Geotechnical Engineering Electronic Journal of Geotechnical Engineering, (Special issue, Bouquet 08) pp. 1-26.

33. Aldrich, C., and Reuter, M.A. (1994) The application of neural nets in the metallurgical industry. Miner. Eng. 7, pp. 793-809.

34. Kanellopoulas, I., and Wilkinson, G.G. (1997) Strategies and best practice for neutral network image classification. Int. J. Remote Sensing. 18, pp. 711-725.

35. Seibi, A., and Al-Alawi, S.M. (1997) Prediction of fracture toughness using artificial neural networks (ANNs). Eng. Fract. Mech. 56, pp. 311-319.

36. Tawadrous, A.S., DeGagne, D., Pierce, M., and Mas Ivars, D. (2009) Prediction of uniaxial compression PFC3D model micro-properties using artificial neural networks. International Journal for Numerical and Analytical methods in Geomechanics. 33, pp.1953-1962.

37. Rumelhart, D.E., Hinton, G.E., Williams, R.J. (1986) Learning internal representation by error propagation. In: Rumelhart, D.E., McClelland, J.L (Ed.), Parallel Distributed Processing. MIT press, Cambridge. pp 318-362.

38. Idris MA, Saiang D, Nordlund E (2012). Consideration of the rock mass property variability in numerical modelling of open stope stability. National Rock Mechanics Day, "Bergmekanikdagen 2012", Stockholm, Sweden. Rock Engineering Research Foundation and National Group ISRM, 2012, pp. 111 – 123.

39. Hammah, R.E., and Yacoub, T.E. (2009) Probabilistic slope analysis with the finite element method. 43rd US Rock Mechanics Symposium and 4th US-Canada Rock Mechanics Symposium, Asheville, ARMA.

40. Hoek, E. and Brown, E.T. (1997) Practical estimates of rock mass strength. Int. J. Rock Mech. Min. Sci. 34, pp. 1165-1186.

41. Sari, M. (2009) The stochastic assessment of strength and deformability characteristics for a pyroclastic rock mass. Int. J. Rock Mech. Min. Sci. 46, pp. 613- 626.

42. Hoek, E., Carranza –Torres, C., and Corkum, B. (2002) Hoek –Brown failure criterion - 2002 edition. In: Proceedings of the 5th North American Rock Mechanics Symposium and 17th Tunnelling Association of Canada Conference: NARMS-TAC 2002, July 7-10, University of Toronto, pp 267-271.

43. Hoek, E., and Diederichs, M.S. (2006) Empirical estimation of rock mass modulus. Int. J. Rock Mech. Min. Sci. 43, pp. 203-215.

44. Palisade Corporation. 2001. @RISK Version 4.0. Available from: www.palisade.com

45. Stephansson, O. (1993) Rock stress in the Fennoscandian shield. In: J.A. Hudson (Editor), Comprehensive Rock Engineering. Pergamon Press, pp. 445-459.

46. Sato, T,, Kikuchi, T. and Sugihara, K. (2000) In-situ experiments on an excavation disturbed zone induced by mechanical excavation in Neogene sedimentary rock at Tono mine, central Japan. Engineering Geology, 56(1-2) pp. 97-108.

47. Lilly, P.A. and Li, J. (2000) Estimating excavation reliability from displacement modeling. Int. J. Rock Mech. Min. Sci. 37, pp. 1261-1265.

48. Sakurai, S. (1981) Direct strain evaluation technique in construction of underground opening. In: Proceedings of 22th US Symp. Rock Mech, MIT, Cambridge, pp 278-282.

49. Sakurai, S. (1986) Field measurement and hazard warning levels in NATM. Soils and Foundation, 34(2) pp. 5-10

50. Sakurai, S. (1997) Lessons learned from field measurements in tunnelling. Tunnelling and Underground Space Technology, 12(4), pp. 453-460.

51. Itasca (2016) FLAC – Fast Langrangian Analysis of Continua, Version 8.0. Available from: www.itascacg.com

52. Fang, K.T. (1980) The uniform design: application of number-theoretic method in experimental design. Acta Math. Appl. Sin. 3, pp. 363-372.

53. Wang, Y., and Fang, K.T. (1981) A note on uniform distribution and experimental design. Chin. Sci. Bull. 26, pp. 485-489.

54. Zhang, L., Liang, Y.Z., Jiang, J.H., Yu, R.Q., and Fang, K.T. (1998) Uniform design applied to nonlinear multivariate calibration by ANN. Anal. Chim. Acta 370 (1), pp. 65-77.

55. Kuo, Y., Yang, T., Peters, B.A., and Chang, I. (2007) Simulation metamodel development systems in semiconductor wafer fabrication. Simul. Model. Pract. Theor. 15 (8), pp. 1002-1015.

56. Cheng, J. and Li, Q.S. (2009) A hybrid artificial neural network method with uniform design for structural optimization. Comput. Mech. 44, pp. 61-71.

57. Sahin, M.A., Jaksa, M.B. and Maier, H.R. (2001) Artificial neural network applications in geotechnical engineering. Australian Geomechanics. 36, pp. 49-62.

58. MATLAB, 2012. Version 2012b. The MathWorks Inc. Available from: www.mathworks.com

59. U.S. Army Corps of Engineers. (1997) Engineering and design introduction to probability and reliability methods for use in geotechnical engineering. Engineering Technical Letter No. 1110-2-547, Department of the Army, Washington, DC.

60. Li, X., Li, X. and Su, Y. (2016) A hybrid approach combining uniform design and support vector machine to probabilistic tunnel stability assessment. Structural safety, 61, pp. 22 – 42.

61. Langford, J.C. (2013) Application of reliability methods to the design of underground structures. Ph.D. Thesis, Queen's University, Canada. pp 512.

62. Rajashekhar, M.R., and Ellingwood, B.R. (1993) A new look at the response surface approach for reliability analysis. Structural Safety, 12, pp. 205-220.

63. Lü, Q., Chan, C.L., and Low, B.K. (2013) System reliability assessment for a rock tunnel with multiple failure modes. Rock Mech Rock Eng, 46, pp. 821-833.

64. Wong, F.S. (1985) First-order, second-moment methods, Computers and Structures, 20(4), pp. 779-791.

Editor's note.
This paper may be referred to, in other articles, as:

Idris, Musa Adebayo, Erling Nordlund, and David Saiang: " Comparison of Different Probabilistic Methods for Analyzing Stability of Underground Rock Excavations" *Electronic Journal of Geotechnical Engineering*, 2016 (21.21), pp 6555-6585. Available at ejge.com.